Tbx1 haploinsufficiency is linked to behavioral disorders in mice and humans: Implications for 22q11 deletion syndrome

Richard Paylor[a,b], Beate Glaser[c,d], Annalisa Mupo[d,e,f,g], Paris Ataliotis[d,h], Corinne Spencer[a,b], Angela Sobotka[e], Chelsey Sparks[e], Chul-Hee Choi[i], John Oghalai[i], Sarah Curran[j], Kieran C. Murphy[k], Stephen Monks[k], Nigel Williams[c], Michael C. O'Donovan[c], Michael J. Owen[c,l], Peter J. Scambler[h], and Elizabeth Lindsay[e,f,m]

Departments of [a]Molecular and Human Genetics, [b]Neuroscience, [e]Pediatrics (Cardiology), and [i]Otolaryngology, Baylor College of Medicine, Houston, TX 77030; [c]Department of Psychological Medicine, Cardiff University, Cardiff CF14 4XN, United Kingdom; [f]CEINGE Biotecnologie Avanzate and [g]European School of Molecular Medicine (SEMM), 80145 Naples, Italy; [h]Molecular Medicine Unit, Institute of Child Health, 30 Guilford Street, London WC1N 1EH, United Kingdom; [k]Department of Psychiatry, Royal College of Surgeons in Ireland, Dublin 9, Ireland; and [j]Department of Psychological Medicine, Institute of Psychiatry, London SE4 8AF, United Kingdom

Edited by Edward M. Scolnick, The Broad Institute, Cambridge, MA, and approved March 10, 2006 (received for review January 9, 2006)

About 35% of patients with 22q11 deletion syndrome (22q11DS), which includes DiGeorge and velocardiofacial syndromes, develops psychiatric disorders, mainly schizophrenia and bipolar disorder. We previously reported that mice carrying a multigene deletion (*Df1*) that models 22q11DS have reduced prepulse inhibition (PPI), a behavioral abnormality and schizophrenia endophenotype. Impaired PPI is associated with several psychiatric disorders, including those that occur in 22q11DS, and recently, reduced PPI was reported in children with 22q11DS. Here, we have mapped PPI deficits in a panel of mouse mutants that carry deletions that partially overlap with *Df1* and have defined a PPI critical region encompassing four genes. We then used single-gene mutants to identify the causative genes. We show that PPI deficits in *Df1*/+ mice are caused by haploinsufficiency of two genes, *Tbx1* and *Gnb1l*. Mutation of either gene is sufficient to cause reduced PPI. *Tbx1* is a transcription factor, the mutation of which is sufficient to cause most of the physical features of 22q11DS, but the gene had not been previously associated with the behavioral/psychiatric phenotype. A likely role for *Tbx1* haploinsufficiency in psychiatric disease is further suggested by the identification of a family in which the phenotypic features of 22q11DS, including psychiatric disorders, segregate with an inactivating mutation of *TBX1*. One family member has Asperger syndrome, an autistic spectrum disorder that is associated with reduced PPI. Thus, *Tbx1* and *Gnb1l* are strong candidates for psychiatric disease in 22q11DS patients and candidate susceptibility genes for psychiatric disease in the wider population.

mouse model | psychiatric disease | DiGeorge syndrome | sensorimotor gating

Caused by a heterozygous multigene deletion, 22q11 deletion syndrome (22q11DS) is a relatively common genetic disorder (1:4,000 live births). Behavioral and psychiatric disorders are a prominent part of the 22q11DS phenotype. In children, these disorders include cognitive defects, anxiety, attention deficit disorder, and problems of social interaction that are increasingly recognized to meet the criteria of autistic spectrum disorder (1, 2), a neurodevelopmental disorder. In adults, high rates of psychotic disorders, especially schizophrenia, have been reported (2–5).

It is likely that the pathophysiological basis of many psychiatric disorders is heterogeneous involving multiple genes and environmental factors. Therefore, when they occur frequently in association with a defined genetic defect, as in the case of 22q11DS (3, 4, 6, 7), it offers a unique opportunity to identify causative or contributing genes, especially if a good animal model is available. We developed a mouse model of 22q11DS (8), the *Df1*/+ mouse, which carries a heterozygous deletion encompassing 22 genes.

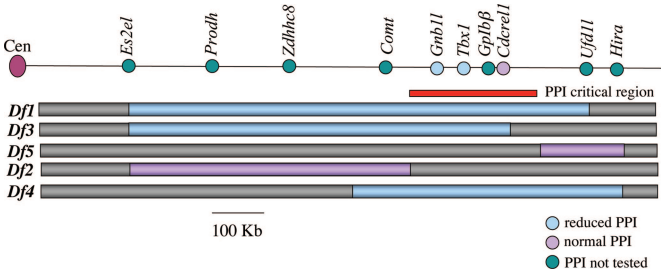

Fig. 1. Deletion mutants and single-gene mutants. The black line at top is a scaled diagram of the mouse chromosome 16 region that is syntenic to human chromosome 22q11.2 showing selected genes. Blue and violet bars below indicate the deletion alleles established in mice. The original nomenclature of these alleles, *Df (16)1–Df (16)5* (13, 14), has been abbreviated to *Df1–Df5*. The red bar indicates the PPI critical region as defined by the deletion mutants. The presence or absence of PPI impairments in mouse mutants is indicated by color, where blue indicates reduced PPI, violet indicates normal PPI, and green indicates PPI not tested.

Df1/+ mice recapitulate many of the cardiovascular defects associated with 22q11DS (8), and they also display abnormal behavior, including impaired sensorimotor gating, as measured by prepulse inhibition (PPI) of the startle response (9), a behavioral abnormality that is associated with several psychiatric and behavioral disorders including schizophrenia and schizotypal personality (reviewed in ref. 10), 22q11DS (11), and Asperger syndrome (12). In the present study, we set out to determine whether reduced PPI in *Df1*/+ mice results from haploinsufficiency of a particular gene or genes. Results unexpectedly revealed the presence of two adjacent, dosage-sensitive genes that significantly affect sensorimotor gating. We also report that psychiatric disorders, in particular Asperger syndrome, can occur in association with inactivating mutations of

Conflict of interest statement: No conflicts declared.

This paper was submitted directly (Track II) to the PNAS office.

Abbreviations: 22q11DS, 22q11 deletion syndrome; PPI, prepulse inhibition; E*n*, embryonic day *n*; ASR, acoustic startle response; VCFS, velocardiofacial syndrome; NLS, nuclear localization signal.

[d]B.G., A.M., and P.A. contributed equally to this work.

[l]To whom correspondence regarding human genetics may be addressed at: Department of Psychological Medicine, Cardiff University, Cardiff CF14 4XN, United Kingdom. E-mail: owenmj@cardiff.ac.uk.

[m]To whom correspondence may be sent at the present address: Institute of Biosciences and Technology, 2121 West Holcombe Boulevard, Houston, TX 77030. E-mail: elindsay@ibt.tamhsc.edu.

GENETICS

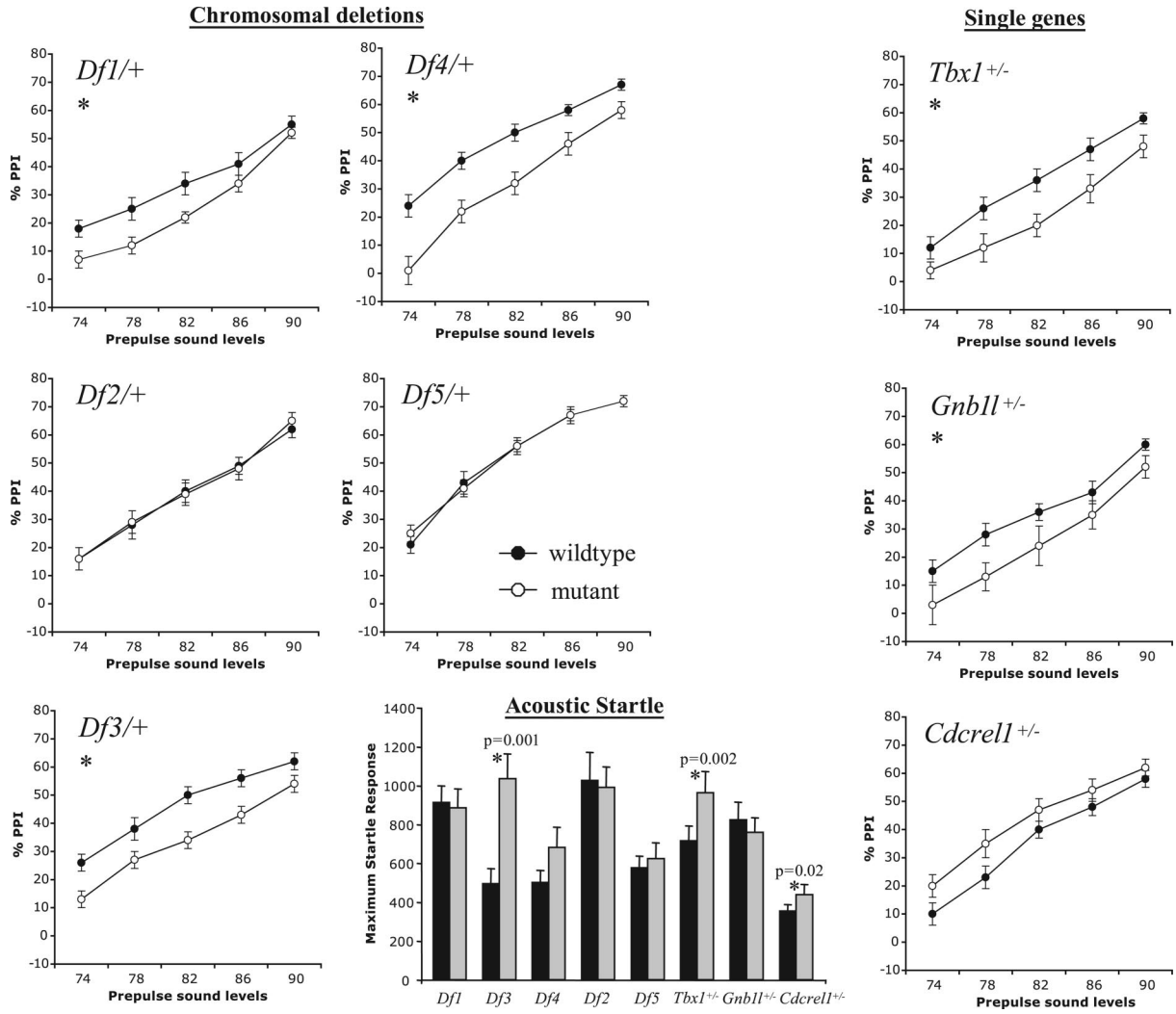

Fig. 2. PPI of the acoustic startle response (ASR). Reduced PPI was seen in deletion mutants *Df1*/+, *Df3*/+, and *Df4*/+ and in *Tbx1*$^{+/-}$ and *Gnb1l*$^{+/-}$ mice. Impairment was most apparent at the lower prepulse sound levels, as previously noted (9). The increased PPI seen in *Cdcrel1*$^{+/-}$ mice did not reach statistical significance. The magnitude of the ASR was significantly greater (*) in *Df3*/+, *Tbx1*$^{+/-}$, and *Cdcrel1*$^{+/-}$ mice than in their respective wild-type littermates, but overall there was no relationship between ASR and PPI.

TBX1, rather than with a 22q11 chromosomal deletion, consistent with our mouse studies.

Results

PPI Analysis of Mouse Mutants. The reflexive response to the acoustic startle stimulus that is the basis of the PPI assay requires that mice can hear, and hearing loss could confound the results of this test. We therefore evaluated auditory function in *Df1*/+ mice by measuring distortion product otoacoustic emissions (for methodology, see *Supporting Text*, which is published as supporting information on the PNAS web site). No difference was found between mutants and wild-type littermates (see Fig. 5, which is published as supporting information on the PNAS web site), indicating that reduced PPI in *Df1*/+ mutants is not secondary to hearing loss.

To identify the gene(s) responsible for impaired sensorimotor gating in *Df1*/+ mice, we performed the PPI assay on five mutant mouse lines (13, 14) that carry heterozygous multigene deletions that are partially overlapping with *Df1* (Fig. 1). All mice analyzed were male and female littermates on a N5–6 C57BL/6$^{c-/c-}$ genetic background that was generated by backcrossing mutant C57BL/6$^{c-/c-}$;129S5/SvEvBrd mice with C57BL/6$^{c-/c-}$ mice for 5–6 generations. Replicating our original observations (9), we found PPI to be significantly impaired in *Df1*/+ mice ($P = 0.044$; Fig. 2). In addition, *Df3*/+ and *Df4*/+ mice also had reduced PPI ($P = 0.004$ and 0.001, respectively), whereas the other two deletion mutants tested, *Df2*/+ and *Df5*/+, had normal PPI ($P = 0.871$ and 0.92, respectively; Fig. 2). Collectively, these results identified a PPI critical region that was defined by the distal *Df2* deletion breakpoint and the proximal *Df5* deletion breakpoint (Fig. 1). The generation of these two chromosomal deletions has been described (13, 14). Briefly, we used retroviral insertion of an *Hprt3′* chromosome engineering cassette (15), using as a substrate for the insertion embryonic stem cell lines in which an *Hprt5′* cassette (15) had been previously inserted into the genes *Es2el* (for *Df2*) and *Hira* (for *Df4* and *Df5*). The proximal *Df5* breakpoint has been localized to the genomic region between *Cdcrel1* and *Cldn1* (14), whereas the distal *Df2* breakpoint had previously only been mapped by *in situ* hybridization by using a large genomic clone. To localize more precisely the *Df2* breakpoint, we used long-range PCR to amplify the breakpoint region (15). Cloning and sequencing of the PCR products identified the breakpoint to be in intron 2 of the *Txnrd2* gene. The published mouse sequence (http://www.ensembl.org) indicated that the refined PPI critical region spanned 300 kb of DNA

and encompassed four genes: *Gnb1l*, *Tbx1*, *Gp1bβ*, and *Cdcrel1* (Fig. 1). Interestingly, this critical region excluded two genes that have been shown to affect PPI in mice, *Prodh* (16) and *Zdhh8c* (17), as being responsible for PPI impairments in the affected deletion mutants. A third candidate behavioral gene that maps within the *Df2* deletion is *Comt*. Several population-based studies have reported genetic association between *COMT* and schizophrenia, although results have been inconsistent. Recently, a *COMT* low-activity allele, *COMT*158met (18), was reported to correlate with increased severity of psychosis and reduced prefrontal cortex gray matter volume in a small longitudinal study of 22q11DS patients (19). Interestingly, in mice, a genetic interaction between *Comt* and *Prodh* has been recently demonstrated (20). Our finding of normal PPI in *Df2*/+ mice, which are heterozygous for *Comt*, is consistent with a previous study that reported normal PPI in $Comt^{+/-}$ and $Comt^{-/-}$ mice (21) and excludes a role for the gene in the *Df1*/+ PPI phenotype.

Genes That Modulate Sensorimotor Gating. To identify the causative gene(s), we performed the PPI assay in $Tbx1^{+/-}$, $Cdcrel1^{+/-}$, and $Gnb1l^{+/-}$ mice. We excluded *GpIbβ* from our analysis because the gene is only expressed in platelets, and in humans *GPIB*B loss of function causes Bernard–Soulier disease, a bleeding disorder that has no known association with psychiatric disease (22). The generation of *Tbx1* and *Cdcrel1* mutants has been reported (13). *Gnb1l* mutant mice were obtained from Lexicon Genetics Inc. (The Woodlands, TX). The *Gnb1l* gene was inactivated by insertion of a gene-trapping cassette into intron 2,476 base pairs upstream of exon 3, which is the first coding exon. The insertion results in aberrant splicing to β-gal and loss of downstream mRNA (data not shown). $Gnb1l^{+/-}$ mice, which were provided on a mixed C57BL/$6^{c-/c-}$;129S5/SvEvBrd background, were healthy and fertile. Loss of *Gnb1l* function is lethal in early embryogenesis, and no $Gnb1l^{-/-}$ embryos were recovered after embryonic day (E)6.5. To test the single-gene mutations on the same background as the deletion mutants, $Tbx1^{+/-}$, $Cdcrel1^{+/-}$, and $Gnb1l^{+/-}$ mice were first backcrossed to C57BL/$6^{c-/c-}$ mice for 5–6 generations. Unexpectedly, the PPI assay showed that both $Tbx1^{+/-}$ and $Gnb1l^{+/-}$ mice had reduced PPI ($P = 0.013$ and 0.046, respectively; Fig. 2), similar to that identified in the affected deletion mutants, whereas $Cdcrel1^{+/-}$ mice were normal ($P = 0.341$). Thus, normal gene dosage of both *Tbx1* and *Gnb1l* is required for normal sensorimotor gating in mice. We conclude that the deletion of these two genes causes impaired sensorimotor gating in *Df1*/+, *Df3*/+, and *Df4* mice. Fig. 2 shows that there were significant increases in the acoustic startle response (ASR) in one of the deletion mutants (*Df3*/+) and in two single-gene mutants, $Tbx1^{+/-}$ and $Cdcrel1^{+/-}$ ($P = 0.001$, 0.002, and 0.02, respectively). Differences in startle responses have been reported between male and female mice, and estrous can affect PPI. However, in the two-way ANOVA for ASR and the three-way ANOVA for PPI, we did not detect a main effect of gender, and more importantly, no gender-specific effect in any of the genotypes. Thus, it is unlikely that the increased ASR in the abovementioned mutants is caused by gender effects. Overall, there was no direct relationship between levels of PPI and acoustic startle amongst the various mutant mouse lines. Such dissociation between PPI and acoustic startle has been documented by others (reviewed in ref. 23).

Brain Expression of *Tbx1* and *Gnb1l*. *Tbx1* encodes a member of the T-box family of transcription factors. We and others have shown that *Tbx1* haploinsufficiency is responsible for cardiovascular, craniofacial, thymic, and parathyroid defects in mouse models of 22q11DS (13, 24, 25), and *TBX1* has been confirmed to be a disease gene through the identification of mutations in patients with a classical 22q11DS phenotype but without the common chromosomal deletion (26). Whether *TBX1* haploinsufficiency is responsible for neurodevelopmental or psychiatric disorders in 22q11DS patients is not known because neuropsychiatric assessments on patients with the three *TBX1* point mutations identified to date have not been reported.

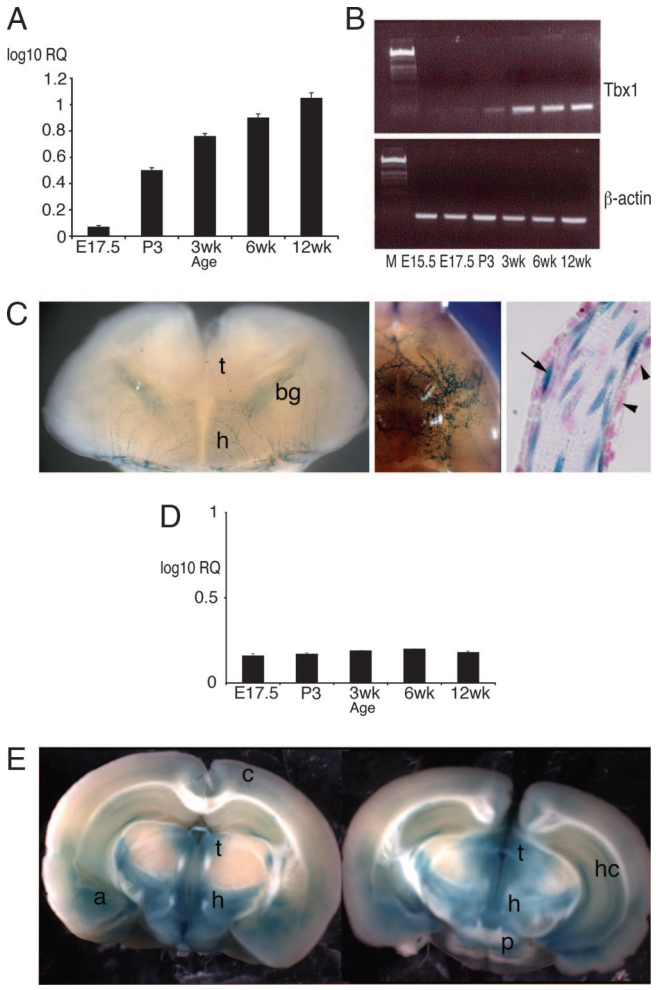

Fig. 3. Brain expression of candidate behavioral genes. *Tbx1* brain expression increases steadily between E17.5 and 12 weeks as measured by real-time quantitative RT-PCR (*A*) and by semiquantitative RT-PCR (*B*). β-Gal staining of a $Tbx1^{+/-}$ embryo at E18.5 (*C*) reveals expression in blood vessels both on the brain surface (*Left* and *Center*) and within the brain parenchyma (*Left*). *Tbx1* is expressed in the endothelial cells lining of blood vessels (arrow in *Right*) but not in the vascular smooth muscle (arrowheads in *Right*). *Gnb1l* expression remains steady at the same developmental stages (*D*). (*E*) β-Gal-stained thick brain sections (coronal) of an adult $Gnb1l^{+/-}$ mouse showing *Gnb1l* expression. bg, basal ganglia; t, thalamus; h, hypothalamus; p, pons; a, amygdala; c, cerebral cortex; hc, hippocampus.

Tbx1 has been shown by RT-PCR to be expressed in postnatal mouse brain (27), but regional brain expression has not been reported. We analyzed *Tbx1* expression at various developmental stages by RT-PCR and real-time quantitative RT-PCR and found it to be very low in preterm embryonic brain, whereas levels increased steadily from birth to 3 months (Fig. 3 *A* and *B*). To analyze regional brain expression we used a lacZ-knockin allele (28), which showed expression to be limited to the vasculature in term embryos (Fig. 3*C*) and in adult mice (not shown). A role for the microvasculature in the pathophysiology of schizophrenia has been proposed on theoretical grounds, because microvascular damage could satisfy developmental and degenerative models of schizophrenia (reviewed in ref. 29). Such a proposal is on the basis of numerous clinical studies that have reported cerebral blood flow abnormalities and increased prevalence of minor physical abnor-

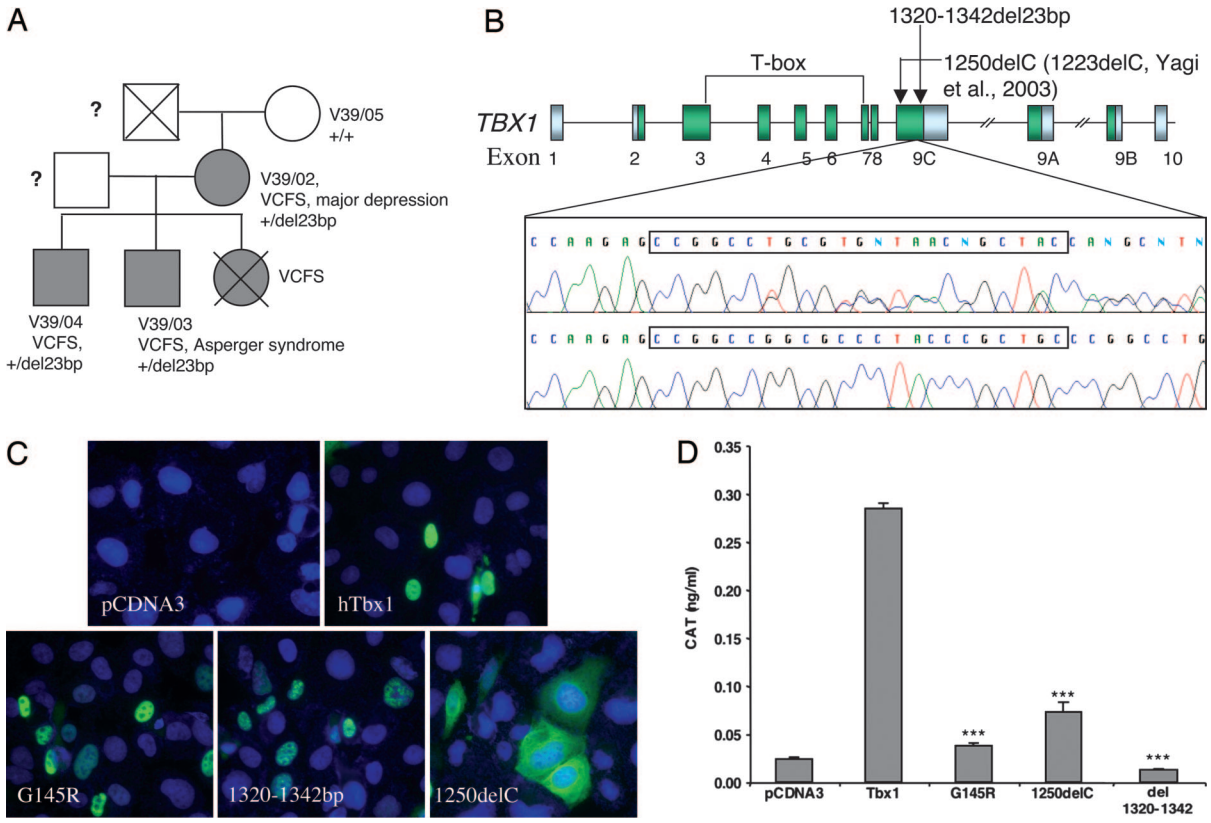

Fig. 4. Patient data and mutation analysis. (*A*) Family of index patient V39/02: Individuals with VCFS are shaded; circles symbolize females; squares symbolize males; and crossed symbols represent deceased family members. ?, no information available. (*B*) Shown at the top is a schematic representation of alternatively spliced *TBX1* transcripts (*TBX1A*, *TBX1B*, *TBX1C*); arrows indicate position of known frameshift mutations in *TBX1C*; green boxes depict *TBX1* coding sequences; and gray boxes depict UTRs. Shown at the bottom is a DNA sequence of a patient with the 1320–1342del23bp mutation (upper panel) and the wild-type *TBX1* sequence in an unrelated individual (lower panel); the position of the mutation is boxed. (*C*) Subcellular localization of wild-type and mutant *TBX1* constructs expressed in U2-OS cells. hTbx1, wild-type TBX1; 1320–1342del, del23bp mutation described here; G145R, predicted null mutation; 1250delC, point mutation described by Yagi *et al.* (26). Constructs were detected with anti-TBX1 antibody. Cell nuclei were stained with DAPI. (*D*) Transcriptional activation of the CAT reporter gene by wild-type and mutant TBX1. Significant differences in transcriptional activation between wild-type TBX1 and a TBX1 construct are indicated by *** ($P \leq 0.001$). Data were normalized for transfection efficiency and depicted as average values ± SEM.

malities in schizophrenia patients and the increased prevalence of schizophrenia in individuals who suffered perinatal problems, especially hypoxia.

Gnb1l encodes an evolutionarily conserved peptide of unknown function, which contains six putative WD40 repeats but no other recognizable functional domains (30, 31). The gene is required for embryonic development and *Gnb1l* loss of function causes embryonic lethality by E6.5 (P.A. and P.J.S., unpublished data). We analyzed *Gnb1l* expression by real-time quantitative RT-PCR and found it to be uniformly expressed between E17.5 and 12 weeks (Fig. 3*D*). The gene is widely expressed in adult mouse brain with striking regional distribution in forebrain, midbrain, and hindbrain structures, including the thalamus, hypothalamus, amygdala, hippocampus, pons (Fig. 3*E*), medulla, and cerebellum (not shown).

Because *Gnb1l* and *Tbx1* lie only 17 kb apart, we considered the possibility that the engineered mutation of either gene may affect expression of its neighbor. We analyzed *Gnb1l* expression in the brain of $Tbx1^{-/-}$ embryos at term by *in situ* hybridization and by real-time quantitative RT-PCR and found no difference between mutant and wild-type littermates (data not shown), indicating that the expression of *Gnb1l* is not regulated by Tbx1 nor is it compromised by the *Tbx1* targeting. The complementary experiment cannot be performed because *Gnb1l* loss of function is lethal before the onset of *Tbx1* expression. However, we have shown that development of the fourth pharyngeal arch artery is a sensitive indicator of *Tbx1* dosage reduction, and 100% of $Tbx1^{+/-}$ embryos has fourth pharyngeal arch artery hypoplasia at E10.5 (32). This phenotype is also observed in embryos heterozygous for a hypomorphic allele of *Tbx1* (33). If the *Gnb1l* targeting were to inactivate *Tbx1*, we would expect to see similar defects in $Gnb1l^{+/-}$ mutants. However, this was not the case and intracardiac ink injection revealed normal fourth pharyngeal arch artery development (data not shown). Although this experiment cannot exclude a tissue-specific effect of *Gnb1l* mutation on *Tbx1* expression in brain, these results make it unlikely that the mutation causes a generalized reduction of *Tbx1* expression.

Mutation Analysis in Patients. The few patients identified so far with *TBX1* mutations have not undergone neuropsychiatric assessment. We have identified a cohort of patients with a 22q11DS-like phenotype but without the common 22q11.2 microdeletion. From this cohort, we selected for mutational analysis of *TBX1* a family with familial velocardiofacial syndrome (VCFS), which is one of the clinical manifestations of 22q11DS (see *Supporting Text* for detailed clinical information). Briefly, the index patient, V39/02 (Fig. 4*A*), has the characteristic facial appearance of VCFS and hypernasal speech. She has no known cardiac defect. Both her surviving children have the characteristic facial appearance of VCFS and congenital heart disease: V39/04, a 17-year-old male, has pulmonary stenosis; and V39/03, a 13-year-old male, was diagnosed at birth with tetralogy of Fallot (Fig. 4*A*). A recent psychiatric assessment of both boys (see *Supporting Text* for methodology)

resulted in the diagnosis of Asperger syndrome in V39/03. Asperger syndrome is an autistic spectrum disorder that is characterized by stereotyped and obsessional behavior and pervasive abnormalities in socioemotional and communicative behavior (34–36). Impaired PPI has been reported in some individuals with Asperger syndrome (12). The presence of Asperger syndrome in a single family member is consistent with the high variability of other features of the 22q11DS, even within families. In addition, psychiatric disorders often appear in adulthood.

Screening of the *TBX1* coding sequence identified a 23-bp frameshift deletion (1320–1342del23bp) in patient V39/02 and in both her sons. The deceased daughter of V39/02 also carried the diagnosis of VCFS, but no DNA was available for analysis. The mutation occurred at the 3′ end of the *TBX1* transcript (counting *A* of the initiation codon as 1; Fig. 4*B*). This mutation was not detected in 716 controls. The frameshift created by 1320–1342del23bp starts at codon 440 in the C terminus of the TBX1 protein and extends the protein from 504 to 616 amino acids. Although the mutation does not affect the T-box, it disrupts the central domain (amino acids 439–448) of a highly conserved nuclear localization signal (NLS) of the wild-type TBX1 protein (37), where it changes the conserved residues PYP to WPR (see Fig. 6, which is published as supporting information on the PNAS web site).

To identify the functional significance of this mutation, we engineered a human *TBX1* cDNA carrying the 1320–1342del23bp mutation and tested the ability of the mutant protein to localize to the nucleus and to transactivate a T-box-binding element construct in a tissue culture system (see *Supporting Text* for methodology). In parallel, we tested two other engineered constructs: 1250delC, which encodes a previously identified mutant form of TBX1 (26), and G145R, which is the equivalent of a loss-of-function TBX5 T-box mutation G80R that prevents DNA binding (38). Immunocytochemical investigation of transfected cells showed tight nuclear localization of the wild-type TBX1 and G145R proteins (Fig. 4*C*), whereas the 1250delC mutant protein was mainly found in the cytoplasm, consistent with the findings of Stoller and Epstein (37) (note that 1250delC in our numbering is equivalent to 1223delC in ref. 26). Unexpectedly, the 1320–1342del23bp mutant protein also localized to the nucleus, despite lacking the NLS (Fig. 4*C*). We therefore examined this peptide sequence for other potential NLS sequences (39) and found that the frameshifted protein contains the sequence RGRRRRCR at amino acids 465–472 (see Fig. 7, which is published as supporting information on the PNAS web site). This sequence corresponds to a known NLS sequence R[GVLIP]RRRRxR that is found in a variety of animal protamine sequences, as well as Epstein–Barr nuclear antigen (http://cubic.bioc.columbia.edu/predictNLS/).

We have shown previously that *TBX1* is a transcriptional activator that can induce expression of a CAT-reporter protein under the control of a Brachyury consensus binding site sequence, 1T-CAT (40). Using the same experimental system, we found that wild-type TBX1 activated the CAT reporter, confirming our previous finding (Fig. 4*D*), whereas the mutant constructs G145R, 1250delC, and 1320–1342del23bp did not. Overall, these data suggest that the mutation identified in V39/02 and her children is a null mutation and that their disease phenotype results from *TBX1* haploinsufficiency.

Discussion

The strong association between common psychiatric disorders and the 22q11.2 microdeletion suggests that haploinsufficiency of one or more genes in the region confers susceptibility to these disorders. Three candidate genes from the region, *COMT*, *PRODH*, and *ZDHH8C*, have been shown to cause behavioral abnormalities when the genes are mutated in mice. PPI defects have been reported in *Prodh* and *Zdhhc8* null mutants (very mild in the latter case), but not in heterozygotes, whereas *Comt* heterozygous and homozygous mice have normal PPI. Our study shows that in a uniform genetic background, combined heterozygosity of all three genes does not affect PPI, although we cannot formally exclude that normal PPI in *Df2/+* mice results from a combined effect of two or more genes that positively and negatively modulate PPI. However, our data are consistent with published data that show normal PPI in *Zdhh8c* and *Comt* heterozygotes [PPI levels have not been reported for *Prodh* heterozygotes, but they have normal L-proline levels (20)]. Thus, in the context of the PPI phenotype, there is no evidence of a genetic interaction between any of these genes at heterozygous gene dosage levels. In the future, it will be interesting to see whether a *Tbx1* transgene can rescue PPI defects in *Df1/+* mutants. Currently, this cannot be tested because the only *Tbx1* transgenic lines available carry transgenes that contain multiple genes, including *Tbx1*.

Our strategy to genetically dissect the *Df1* deletion unexpectedly revealed the presence of two adjacent, dosage-sensitive genes that significantly affect sensorimotor gating. Several genes are known to affect sensorimotor gating, and PPI defects are genetically heterogeneous. Importantly from the disease perspective however, *Tbx1* and *Gnb1l* represent previously unrecognized examples of genes that affect PPI in the heterozygous mutant state. Both genes are hemizygous in 22q11DS patients, making them strong candidates for the associated psychiatric and behavioral phenotypes. The two genes are apparently unrelated and have distinct expression patterns in brain, suggesting that they are unlikely to function in the same genetic pathway. Particularly intriguing is our finding of an inactivating mutation in *TBX1* in an individual with Asperger syndrome. Because of the small number of patients identified so far with *TBX1* mutations, it is difficult to evaluate the relative contribution of *TBX1* haploinsufficiency to behavioral disorders and psychiatric disease in 22q11DS. However, our mouse studies show that of 22 genes tested, *Tbx1* and *Gnb1l* are the only ones that cause PPI impairment in the heterozygous state. Therefore, we propose that these two genes are major contributors to the 22q11DS psychiatric phenotype. Furthermore, we propose that in the general population, the 88-kb genomic segment region that harbors *TBX1* and *GNB1L* may represent a susceptibility locus for schizophrenia and other psychiatric disorders characterized by PPI impairment. Future studies into the functions of these two genes in brain should clarify the genetic pathways affected by their mutation and, potentially, may lead to the identification of drug targets aimed at prevention and or treatment of the psychiatric symptoms in 22q11DS patients. Of particular interest is the observation that *Tbx1* expression in brain increases postnatally, suggesting that early drug intervention may prevent the onset of *Tbx1*-related psychiatric disorders.

Methods

Mouse Strains, Breeding, and Genotyping. Behavioral testing was performed on a total of 502 mice (n = 25–35 mutant and wild-type male and female littermates for each mutation). For each genotype, similar numbers of males and females were tested. The mice were all on a N5–6 C57BL/$6^{c-/c-}$ genetic background generated by backcrossing C57BL/$6^{c-/c-}$;129S5/SvEvBrd mixed-background mutant mice with C57BL/$6^{c-/c-}$ mice for 5–6 generations. *Gnb1l*$^{+/-}$ mice were provided by Lexicon Genetics Inc., and were generated by blastocyst injection of stem cells from OST35527 (OmniBank). Mice were genotyped by PCR by using DNA extracted from tail biopsies (see *Supporting Text* for primer sequences).

PPI Assay. PPI was measured by using the SR-Lab system (San Diego Instruments, San Diego) as described (41). Animals were tested at age 8–16 weeks. Before testing, each mouse was acclimatized to the Plexiglas cylinder for 5 min, during which time the background noise level (70 dB) was continually present. Individual mice were then exposed to six blocks of seven trial types that were presented in a pseudorandom order with an average intertrial

interval of 15 seconds. The seven trial types comprised the following: trial 1 (startle-only trial), 40 ms, 120 dB sound burst; trials 2–6 (prepulse trials), 120 dB startle stimulus preceded 100 ms by 20 ms prepulse sounds of 74, 78, 82, 86, or 90 dB; and trial 7, 70 dB background noise. The startle response was recorded for 65 ms, measuring every 1 ms from the onset of the startle stimulus. The maximum startle amplitude recorded during the 65-ms sampling window was used as the dependent variable. We calculated % PPI as: 100 – [(startle response on acoustic prepulse plus startle stimulus trials/startle response-alone trials) × 100]. Data for each deletion and mutation were analyzed independently. Acoustic response amplitude data were analyzed by using two-way (genotype × gender) ANOVAs. PPI data were analyzed by using a three-way (genotype × gender × prepulse sound level) ANOVA with repeated measures.

Gene Expression Analyses. To visualize β-gal activity, 4% paraformaldehyde-fixed brains were stained in X-gal substrate according to standard procedures. Two- to 3-mm-thick brain sections were photographed as whole-mount specimens and then embedded in paraffin. Sections (10 μm) were counterstained with Nuclear Fast Red. RNA *in situ* hybridization was performed on 10-μm 4% paraformaldehyde-fixed sections (42). Labeled sense and antisense RNA probes were prepared by reverse transcription of DNA clones in the presence of ^{35}S-UTP (MP Biomedicals, Irvine, CA).

Control Subjects. Unrelated British Caucasian control subjects were recruited from the Blood Transfusion Service in Wales and England (482 males and 234 females; mean age 41.5 years, SD ± 11.5 years). The sample was not specifically screened for psychiatric illness, but subjects were not taking regular prescribed medications.

Mutation Detection and Sequencing. A transcript map of *TBX1* was created by using the Golden Path Genome Browser (May 2004 freeze) (http://genome.ucsc.edu/). The coding sequence of the *TBX1* isoform C [National Center for Biotechnology Information (NCBI) accession no. NM_080647], *TBX1* isoform B (NCBI accession no. NM_005992), and *TBX1* isoform C (NCBI accession no. NM_080646, NCBI) and at least 50 bp of intronic sequence adjacent to each exon were screened for sequence variants in patient V39/02. Primers were constructed by using the PRIMER3 program (http://www.genome.wi.mit.edu/cgi-bin/primer/primer3_www.cgi). Mutation detection analysis was performed by denaturing high-performance liquid chromatography (43). All samples with heteroduplex traces were subsequently sequenced with BigDye Terminator 3.0 cycle sequencing kit and analyzed on an ABI3100 sequencer (PE Applied Biosystems).

Genotyping of* TBX1 *deletions. The identified deletion was typed by using 5′-fluorescently labeled PCR primers (FAM dye), and PCR products were resolved on an ABI3100 sequencer. The data were analyzed with GENESCAN 3.7 and GENOTYPER 2.5 software.

CAT assays. U2-OS cells were grown in 12-well dishes to 90% confluency and transfected in quadruplicate with Lipofectamine 2000 (Invitrogen). The 1T-CAT reporter construct (44) was cotransfected with *TBX1* DNA and the β-gal expression vector, pCH110 (Amersham Pharmacia), which was used for normalization. The concentration of CAT protein in cell lysates was determined by using the CAT-ELISA kit (Roche). Differences in transcriptional activation between wild-type and mutant *TBX1* constructs were evaluated by using a Kruskal–Wallis test (SPSS, Chicago) because the assumption of normality for the variable transcriptional activation was not given.

Immunocytochemistry. U2-OS cells were grown on poly(D-lysine)-coated glass coverslips to 90% confluency and transfected as before with *TBX1* constructs in pCDNA3. Cells were fixed in 4% paraformaldehyde after 24 h and permeabilized with 0.05% Nonidet P-40 in PBS. Cells were incubated with rabbit anti-*Tbx1* antibody (Zymed) at 1:100 then with donkey anti-rabbit IgG Alexa Fluor 488 (Molecular Probes) at 1:200. Cells were mounted in Vectashield (Vector Laboratories) with DAPI and photographed by using a Zeiss AxioVision microscope.

We thank M. Reese, P. Terrell, G. Ji, and C. Gerken for technical support and S. Reed for clinical assistance. This work is supported by the National Institutes of Health, National Institutes of Mental Health (E.L. and R.P.), the March of Dimes (E.L.), and the Ministero dell'Instruzione, dell'Università e della Ricerca (E.L.). This work was also supported by the Mental Retardation and Developmental Disabilities Research Center Neurobehavioral Core, Baylor College of Medicine. E.L. is an Associate Telethon Scientist. P.A. and P.J.S. were supported by the British Heart Foundation and the Health Foundation. K.C.M., N.W., M.C.O., and M.J.O. were supported by a grant from the Wellcome Trust. *Gnbl1* mutant mice were generated by and purchased from Lexicon Genetics Inc.

1. Fine, S. E., Weissman, A., Gerdes, M., Pinto-Martin, J., Zackai, E. H., McDonald-McGinn, D. M. & Emanuel, B. S. (2005) *J. Autism Dev. Disord.* **35,** 461–470.
2. Niklasson, L., Rasmussen, P., Oskarsdottir, S. & Gillberg, C. (2001) *Genet. Med.* **3,** 79–84.
3. Bassett, A. S., Hodgkinson, K., Chow, E. W., Correia, S., Scutt, L. E. & Weksberg, R. (1998) *Am. J. Med. Genet.* **81,** 328–337.
4. Murphy, K. C., Jones, L. A. & Owen, M. J. (1999) *Arch. Gen. Psychiatry* **56,** 940–945.
5. Bassett, A. S., Chow, E. W., AbdelMalik, P., Gheorghiu, M., Husted, J. & Weksberg, R. (2003) *Am. J. Psychiatry* **160,** 1580–1586.
6. Shprintzen, R. J., Goldberg, R., Golding-Kushner, K. J. & Marion, R. W. (1992) *Am. J. Med. Genet.* **42,** 141–142.
7. Lindsay, E. A., Morris, M. A., Gos, A., Nestadt, G., Wolyniec, P. S., Lasseter, V. K., Shprintzen, R., Antonarakis, S. E., Baldini, A. & Pulver, A. E. (1995) *Am. J. Hum. Genet.* **56,** 1502–1503.
8. Lindsay, E. A., Botta, A., Jurecic, V., Carattini-Rivera, S., Cheah, Y.-C., Rosenblatt, H. M., Bradley, A. & Baldini, A. (1999) *Nature* **401,** 379–383.
9. Paylor, R., McIlwain, K. L., McAninch, R., Nellis, A., Yuva-Paylor, L. A., Baldini, A. & Lindsay, E. A. (2001) *Hum. Mol. Genet.* **10,** 2645–2650.
10. Braff, D. L., Geyer, M. A. & Swerdlow, N. R. (2001) *Psychopharmacology (Berlin)* **156,** 234–258.
11. Sobin, C., Kiley-Brabeck, K. & Karayiorgou, M. (2005) *Am. J. Psychiatry* **162,** 1090–1099.
12. McAlonan, G. M., Daly, E., Kumari, V., Critchley, H. D., van Amelsvoort, T., Suckling, J., Simmons, A., Sigmundsson, T., Greenwood, K., Russell, A., *et al.* (2002) *Brain* **125,** 1594–1606.
13. Lindsay, E. A., Vitelli, F., Su, H., Morishima, M., Huynh, T., Pramparo, T., Jurecic, V., Ogunrinu, G., Sutherland, H. S., Scambler, P. J., *et al.* (2001) *Nature* **410,** 97–101.
14. Vitelli, F., Lindsay, E. A. & Baldini, A. (2002) *Cold Spring Harbor Symp. Quant. Biol.* **67,** 327–332.
15. Su, H., Wang, X. & Bradley, A. (2000) *Nat. Genet.* **24,** 92–95.
16. Gogos, J. A., Santha, M., Takacs, Z., Beck, K. D., Luine, V., Lucas, L. R., Nadler, J. V. & Karayiorgou, M. (1999) *Nat. Genet.* **21,** 434–439.
17. Mukai, J., Liu, H., Burt, R. A., Swor, D. E., Lai, W. S., Karayiorgou, M. & Gogos, J. A. (2004) *Nat. Genet.* **36,** 725–731.
18. Chen, J., Lipska, B. K., Halim, N., Ma, Q. D., Matsumoto, M., Melhem, S., Kolachana, B. S., Hyde, T. M., Herman, M. M., Apud, J., *et al.* (2004) *Am. J. Hum. Genet.* **75,** 807–821.
19. Gothelf, D., Eliez, S., Thompson, T., Hinard, C., Penniman, L., Feinstein, C., Kwon, H., Jin, S., Jo, B., Antonarakis, S. E., *et al.* (2005) *Nat. Neurosci.* **8,** 1500–1502.
20. Paterlini, M., Zakharenko, S. S., Lai, W. S., Qin, J., Zhang, H., Mukai, J., Westphal, K. G., Olivier, B., Sulzer, D., Pavlidis, P., *et al.* (2005) *Nat. Neurosci.* **8,** 1586–1594.
21. Gogos, J. A., Morgan, M., Luine, V., Santha, M., Ogawa, S., Pfaff, D. & Karayiorgou, M. (1998) *Proc. Natl. Acad. Sci. USA* **95,** 9991–9996.
22. Budarf, M. L., Konkle, B. A., Ludlow, L. B., Michaud, D., Li, M., Yamashiro, D. J., McDonald-McGinn, D., Zackai, E. H. & Driscoll, D. A. (1995) *Hum. Mol. Genet.* **4,** 763–766.
23. Geyer, M. A., McIlwain, K. L. & Paylor, R. (2002) *Mol. Psychiatry* **7,** 1039–1053.
24. Merscher, S., Funke, B., Epstein, J. A., Heyer, J., Puech, A., Min Lu, M. M., Xavier, R. J., Demay, M. B., Russell, R. G., Factor, S., *et al.* (2001) *Cell* **104,** 619–629.
25. Jerome, L. A. & Papaioannou, V. E. (2001) *Nat. Genet.* **27,** 286–291.
26. Yagi, H., Furutani, Y., Hamada, H., Sasaki, T., Asakawa, S., Minoshima, S., Ichida, F., Joo, K., Kimura, M., Imamura, S., *et al.* (2003) *Lancet* **362,** 1366–1373.
27. Maynard, T. M., Haskell, G. T., Peters, A. Z., Sikich, L., Lieberman, J. A. & LaMantia, A. S. (2003) *Proc. Natl. Acad. Sci. USA* **100,** 14433–14438.
28. Vitelli, F., Morishima, M., Taddei, I., Lindsay, E. A. & Baldini, A. (2002) *Hum. Mol. Genet.* **11,** 915–922.
29. Hanson, D. R. & Gottesman, I. I. (2005) *BMC Med. Genet.* **6,** 7.
30. Gong, L., Liu, M., Jen, J. & Yeh, E. T. (2000) *Biochim. Biophys. Acta* **1494,** 185–188.
31. Funke, B., Pandita, R. K. & Morrow, B. E. (2001) *Genomics* **73,** 264–271.
32. Lindsay, E. A. & Baldini, A. (2001) *Hum. Mol. Genet.* **10,** 997–1002.
33. Xu, H., Morishima, M., Wylie, J. N., Schwartz, R. J., Bruneau, B. G., Lindsay, E. A. & Baldini, A. (2004) *Development (Cambridge, U.K.)* **131,** 3217–3227.
34. Gillberg, C. (1998) *Br. J. Psychiatry* **172,** 200–209.
35. Gillberg, C., Rastam, M. & Wentz, E. (2001) *Autism* **5,** 57–66.
36. Wing, L. (2005) *J. Autism Dev. Disord.* **35,** 197–203.
37. Stoller, J. Z. & Epstein, J. A. (2005) *Hum. Mol. Genet.* **14,** 885–892.
38. Basson, C. T., Huang, T., Lin, R. C., Bachinsky, D. R., Weremowicz, S., Vaglio, A., Bruzzone, R., Quadrelli, R., Lerone, M., Romeo, G., *et al.* (1999) *Proc. Natl. Acad. Sci. USA* **96,** 2919–2924.
39. Cokol, M., Nair, R. & Rost, B. (2000) *EMBO Rep.* **1,** 411–415.
40. Ataliotis, P., Ivins, S., Mohun, T. J. & Scambler, P. J. (2005) *Dev. Dyn.* **232,** 979–991.
41. Paylor, R. & Crawley, J. N. (1997) *Psychopharmacology (Berlin)* **132,** 169–180.
42. Albrecht, U., Eichele, G., Helms, J. A. & Lu, H. C. (1997) in *Molecular and Cellular Methods in Developmental Toxicology*, ed. Daston, G. P. (CRC, New York), pp. 23–48.
43. Jones, A. C., Austin, J., Hansen, N., Hoogendoorn, B., Oefner, P. J., Cheadle, J. P. & O'Donovan, M. C. (1999) *Clin. Chem.* **45,** 1133–1140.
44. Conlon, F. L., Sedgwick, S. G., Weston, K. M. & Smith, J. C. (1996) *Development (Cambridge, U.K.)* **122,** 2427–2435.